ATM regulates the length of individual telomere tracts in *Arabidopsis*

Laurent Vespa[†], Ross T. Warrington[†], Petr Mokros[‡], Jiri Siroky[‡], and Dorothy E. Shippen[†§]

[†]Department of Biochemistry and Biophysics, Texas A&M University, College Station, TX 77843-2128; and [‡]Department of Plant Developmental Genetics, Institute of Biophysics, Academy of Sciences of the Czech Republic, Kralovopolska 135, 61265 Brno, Czech Republic

Edited by Carol W. Greider, Johns Hopkins University School of Medicine, Baltimore, MD, and approved October 1, 2007 (received for review May 11, 2007)

Telomeres have the paradoxical ability of protecting linear chromosome ends from DNA damage sensors by using these same proteins as essential components of their maintenance machinery. We have previously shown that the absence of ataxia telangiectasia mutated (ATM), a central regulator of the DNA damage response, accelerates the onset of genome instability in telomerase-deficient *Arabidopsis*, without increasing the rate of bulk telomere shortening. Here, we examine individual telomere tracts through successive plant generations using both fluorescence *in situ* hybridization (FISH) and primer extension telomere repeat amplification (PETRA). Unexpectedly, we found that the onset of profound developmental defects and abundant end-to-end chromosome fusions in fifth generation (G_5) *atm tert* mutants required the presence of only one critically shortened telomere. Parent progeny analysis revealed that the short telomere arose as a consequence of an unusually large telomere rapid deletion (TRD) event. The most dramatic TRD was detected in *atm tert* mutants that had undergone meiosis. Notably, in contrast to TRD, alternative lengthening of telomeres (ALT) was suppressed in the absence of ATM. Finally, we show that size differences between telomeres on homologous chromosome ends are greater for *atm tert* than *tert* plants. Altogether, these findings suggest a dual role for ATM in regulating telomere size by promoting elongation of short telomeres and by preventing the accumulation of cells that harbor large telomere deletions.

chromosome | homologous recombination | telomerase | alternative lengthening of telomeres | telomere rapid deletion

Telomeres impart stability to the genome by compensating for replicative and enzymatic resection of chromosome ends and by preventing the DNA damage response machinery from recognizing telomeres as double-strand breaks. Composed of G-rich repeat sequences, the telomeric DNA tract terminates in a single-strand 3′ overhang that can fold back upon itself to invade the duplex region and form a t-loop. Telomeric DNA is bound by a set of specific proteins that constitute the shelterin complex (1). TRF2, a core shelterin component is implicated in the stabilization of the t-loop (2). Although telomere length varies among different organisms, it is constrained within a tightly defined size range dictated through shelterin interactions with telomerase. A molecular switch renders long telomeres resistant to telomerase action whereas short telomeres are selectively accessible to telomerase (3). Telomere length regulation is crucial as critically shortened telomeres lead to activation of a DNA damage response and ultimately to end-to-end chromosome fusion (4).

Chromosome ends are also subjected to recombination. In the absence of telomerase, telomeres can be elongated by homologous recombination, a phenomenon termed alternative lengthening of telomeres (ALT) (5, 6). Counterbalancing telomere elongation reactions is telomere rapid deletion (TRD), an intrachromatid recombinational mechanism that culminates in a sudden loss of large portions of telomeric tracts (7). Current models propose that TRD is facilitated by branch migration of the d-loop structure embedded within the t-loop, giving rise to a recombination intermediate resembling a Holliday junction (8). Resolution of the Holliday junction produces a truncated telomere and an extrachromosomal circle of telomeric DNA. The incidence of TRD is dramatically increased at grossly elongated telomeres; in a single step, the extended telomere is brought down to the expected wild type length (6, 9). In yeast, TRD occurs during mitosis, but more precise length resetting is accomplished in meiosis (9–11). Meiotic telomere resetting depends on alignment of homologous chromosomes during prophase I; altering bouquet formation impairs this process (10). Thus, TRD is postulated to serve as a potent telomere resizing mechanism that coordinates the length of telomere tracts on homologous chromosomes (11).

In yeast, TRD depends on the non-nucleolytic activity of Mre11 and Rad50, components of the Mre11 Rad50 Xrs2/Nbs1 (MRX/N) DNA repair complex (12). In higher eukaryotes, large deletions of t-loop sizes are associated with depletion of TRF2 from human cells (13). Telomere deletions are dependent on the Holliday junction resolvase XRCC3 as well as on Nbs1, the homolog of Xrs2 (13, 14), implicating MRN in mammalian TRD. Furthermore, recent studies indicate that human telomeres undergo a transient DNA damage response in S/early G_2 phase of the cell cycle, which is linked to the recruitment of MRN and the PI3-like protein kinases ataxia telangiectasia mutated (ATM) and ataxia telangiectasia and Rad3-related (ATR) (15, 16). This response may promote t-loop formation after passage of the replication fork, and illustrates the shifting equilibrium of functions performed by telomere-associated DNA repair proteins (17, 18).

Here, we focus on the role of ATM in telomere dynamics. ATM is a central regulator of the DNA damage response, inducing a cell cycle checkpoint upon detection of deleterious double-strand breaks (19). In *Arabidopsis*, ATM is essential for the transcriptional up-regulation of more than a hundred genes after DSB-inducing treatment (20). ATM interacts with components of shelterin (21, 22), and in yeast and mammals is required for telomere length regulation. Loss of mammalian ATM or its yeast homolog Tel1p results in shorter but relatively stable telomere tracts (23, 24).

ATM is also implicated in chromosome end protection. Short telomeres are more prone to fusion in yeast and mammalian telomerase mutants lacking ATM (25–27). A similar telomere deprotection phenomenon has been reported for ATM deficient *Drosophila* (28, 29). Previously, we showed that bulk telomere length in *Arabidopsis* is unaffected by the loss of ATM. However,

Author contributions: L.V. and D.E.S. designed research; L.V., R.T.W., P.M., and J.S. performed research; L.V., R.T.W., J.S., and D.E.S. analyzed data; and L.V. and D.E.S. wrote the paper.

The authors declare no conflict of interest.

This article is a PNAS Direct Submission.

Freely available online through the PNAS open access option.

[§]To whom correspondence should be addressed. E-mail: dshippen@tamu.edu.

This article contains supporting information online at www.pnas.org/cgi/content/full/0704466104/DC1.

plants doubly deficient for ATM and TERT, the catalytic subunit of telomerase, display an early onset of developmental defects and severe genome instability, becoming completely sterile in the fifth generation (G_5) of the mutant (30). In contrast, *tert* mutants do not display this terminal phenotype until G_8 (31). Notably, mice doubly deficient in ATM and telomerase also show an early onset of genome instability (25, 26). This defect has been proposed to reflect ATM's function in the DNA damage checkpoint that is activated when telomeres become critically shortened. Alternatively, ATM may play a more direct role at chromosome termini by protecting the shortest telomeres from being recruited into end-joining reactions (4).

To further investigate the role of ATM in telomere biology, we examined the dynamics of individual telomere tracts in *Arabidopsis atm tert* mutants. Here, we show that genome instability in G_5 *atm tert* is instigated by a single critically shortened telomere, which arose as a consequence of TRD. Unusually large deletion events were associated with *atm tert* parents and their progeny, implicating ATM in telomere length regulation. We also found an increased incidence of ALT during somatic development of *tert*, but not *atm tert*, implying that ATM promotes ALT. Finally, in the absence of ATM, the size range of telomeres on homologous chromosome ends was significantly larger than in *tert* mutants, arguing that ATM is involved in regulating telomere length on homologous chromosomes. We conclude that ATM makes several distinct contributions to the regulation of telomere length on individual chromosome ends.

Results

Overrepresentation of a Single Chromosome End at Fusion Junctions in *atm tert*. To investigate the underlying mechanism for the early onset of the terminal phenotype in *atm tert* mutants, we examined the sequence composition of DNA in chromosome fusion junctions by FISH using a series of unique subtelomeric BACs specific for each chromosome end (32). G_5 *atm tert* mutants derived from three independent lines (D3, D5 and F11) were monitored. In each line, several plants showed severe growth defects and in these mutants ≈10–30% of the anaphases displayed bridged chromosomes. Although hybridization signals were detected at the majority of anaphase bridges, there was a strong bias for involvement of a single chromosome end in each line. For line D5, 62% (28/45) anaphase bridges contained 1L DNA (Fig. 1 *A* and B; Table 1), whereas in lines D3 and F11, 100% (17/17 and 27/27 of the bridges, respectively), contained 25S rDNA (Fig. 1 *C* and *D*; Table 1). Because 2L and 4L telomeres are directly abutted by nucleolar organization regions (NORs) (33), both of these chromosome ends are detected by the 25S probe. Subsequent FISH analysis using a 5S rDNA probe confirmed that all of the anaphase bridges in F11 involved the 4L telomere (Fig. 1 *C* and *D*). We suspect that the inability to detect the 1L terminus in all of the fusion junctions in *atm tert* line D5 reflects the lower sensitivity of this probe. Unlike the bridges in lines F11 and D3, which hybridized to megabase regions of repetitive rDNA repeats, anaphase bridges in line D5 were detected by a unique BAC probe to 1L encompassing ≈100 kb.

Consistent with the involvement of a single chromosome end, FISH revealed striking symmetry in the anaphase bridges in all three lines of *atm tert* mutants (Fig. 1 *A–D*). In the large majority of bridges, the hybridization signal was equally distributed on either side of the midline. This observation, coupled with the presence of a second signal outside of the bridge for the other homolog (Fig. 1 *A* and *B*), indicates that chromosome fusions involve sister chromatids. Hence, our inability to recover telomere fusion PCR products from G_5 *atm tert* mutants (30) may be due to the giant palindromes created by sister chromatid fusion that would prohibit amplification by PCR.

In contrast to *atm tert*, anaphase bridges in G_6 and G_8 *tert* plants reflect fusion of many different chromosomes (Fig. 1 *E* and *F*; Table 1; refs. 32 and 34). In G_6 *tert* line 69, DNA from seven different chromosome ends was detected in anaphase bridges (Table 1; ref. 32). Interestingly, telomeric DNA was associated with the majority of fusion junctions in G_6 *tert* mutants (line 69), but was rarely detected in G_5 *atm tert* line D5 (Fig. 1 *G* and *H*; data not shown). To monitor overall genome integrity in *atm tert* mutants, we examined the number of centromeric DNA signals in interphase cells (Table 2). As expected, G_8 *tert* mutants exhibited a high level of aneuploidy with 52% of the cells showing an abnormal number of centromeric DNA signals. In contrast, G_5 *atm tert* mutants, despite their severe defects in growth and development, displayed approximately the same level of aneuploidy as G_6 *tert* mutants, which are wild type in appearance (Table 2). We conclude that ATM inactivation in a telomerase mutant does not promote gross genome rearrangements involving multiple chromosomes.

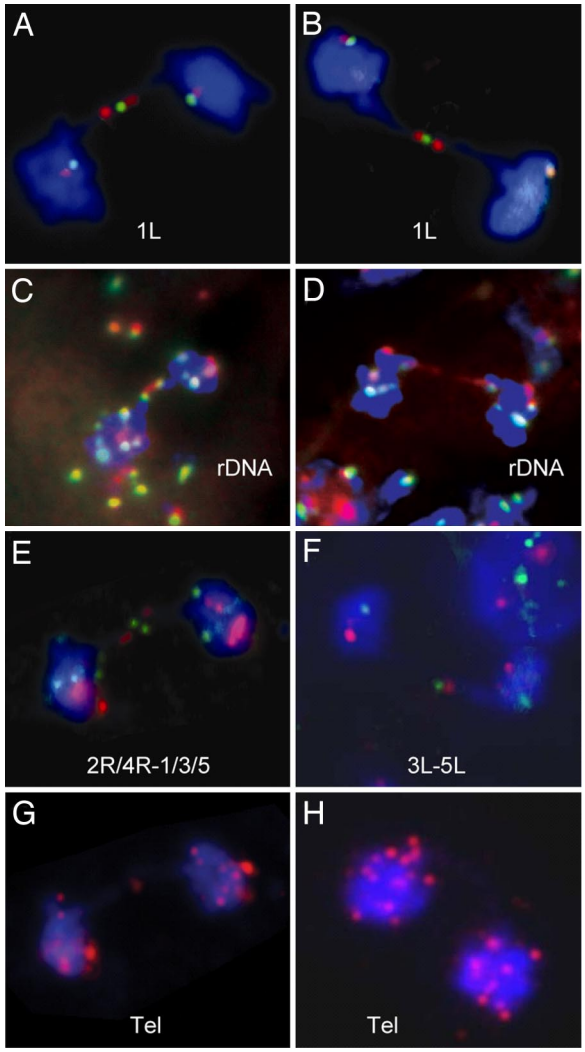

Fig. 1. Overrepresentation of a single chromosome end at anaphase bridges in G_5 *atm tert*. Mitotic cells from pistils were subjected to FISH using probes for unique subtelomeric DNA sequences or telomeric DNA. (*A* and *B*) Detection of the 1L subtelomere at a chromosome fusion junction in G_5 *atm tert* line D5. Hybridization with a distal subtelomeric probe (close to the telomere) is shown in green and a proximal subtelomeric probe (away from the telomere) in red. (*C* and *D*) 4L fusion in G_5 *atm tert* line F11. Red signals correspond to 25S rDNA and green to 5S rDNA. The 5S rDNA probe hybridizes to 3R, 4L, and 5R, implicating the 4L NOR telomere in this fusion. (*E* and *F*) Chromosome fusions involving two different chromosome ends in G_6 *tert*. (*E*) A mixture of eight probes corresponding to all chromosome ends except 2L and 4L was used. Fusions involve 2R or 4R (green) and either end of chromosome 1, 3, or 5 (red). (*F*) A bridge between 3L (green) and 5L (red). (*G* and *H*) FISH with a telomeric DNA probe for a G_6 *tert* mutant (*G*), and a G_5 *atm tert* mutant (*H*) is shown.

Table 1. Characterization of chromosome fusion junctions in *tert* and *atm tert* by FISH

Mutant	Line	Total anaphases counted	Total fusion events	Subtelomeric DNA at junction*
tert G_6	Ref. 32	3,414	174	2L: 30% 3L: 30% 4L: 29% 3R: 15% 4R: 5% 1R: 4% 5L: 2%
tert G_6	69	1,258	39	2L or 4L: 5 (13%) Other: 34 (87%)
tert G_8	69	208	72	2L or 4L: 35 (49%) Other: 53 (74%)
atm tert G_5	D5	157	45	2L or 4L: 0 1L: 28 (62%) Other: 0
atm tert G_5	F11†	92	27	4L: 27 (100%)
atm tert G_5	D3†	76	17	2L: 17 (100%)

*Percentages do not total 100% because junctions may be composed of two different chromosome ends.
†For *atm tert* lines F11 and D3, the involvement of 4L or 2L was determined by the presence or absence, respectively, of 5S rDNA at the junction (see Fig. 1).

A Single Critically Shortened Telomere in G_5 *atm tert* mutants. To determine whether the onset of chromosome fusions in G_5 *atm tert* mutants correlated with the presence of a critically shortened telomere, PETRA (34) was used to measure the length of individual telomeres. PETRA is a PCR-based technique that amplifies specific telomere tracts using a primer directed at the G-overhang and a unique subtelomeric primer. Although PETRA occasionally failed with the 4L or 5R primer, in most experiments we monitored 9/10 *Arabidopsis* chromosome ends. G_5 and G_6 *tert* mutants (lines C4 and C9) derived from the same $atm^{+/-}$ $tert^{+/-}$ parent used to establish the D5, D3, and F11 lines produced a sharp banding pattern of PETRA products (Fig. 2*A*). Occasionally, a particular telomere was represented by two or three discrete bands; such products seem to correspond to homologous chromosomes that may or may not have been subjected to TRD or ALT (see below). The sharpness of the bands is consistent with the loss of length heterogeneity associated with a telomerase deficiency (31). As expected from their wild type phenotype and the absence of anaphase bridges in these plants, all of the telomere tracts were well above the 300-bp threshold, the minimal functional length of an *Arabidopsis* telomere (34).

For plants displaying a terminal phenotype in two of three G_5 *atm tert* lines we found one exceptionally short telomere (Fig. 2*B*). For line D5, analysis of three sibling plants revealed that the 1L telomeres was the shortest overall, with a telomere signal corresponding to only 360 bp in length. Similarly, terminal plants in line D3, gave rise to a faint signal for the 2L telomere corresponding to only 350 bp (Fig. 2*B*). We note that the 1L and 2L telomeres account for the vast majority of chromosome end-joining events in the D5 and D3 lines, respectively (Fig. 1). Based on FISH, we suspect that the F11 *atm tert* line bears a very short 4L telomere, but we were unable to reproducibly amplify PETRA products with this

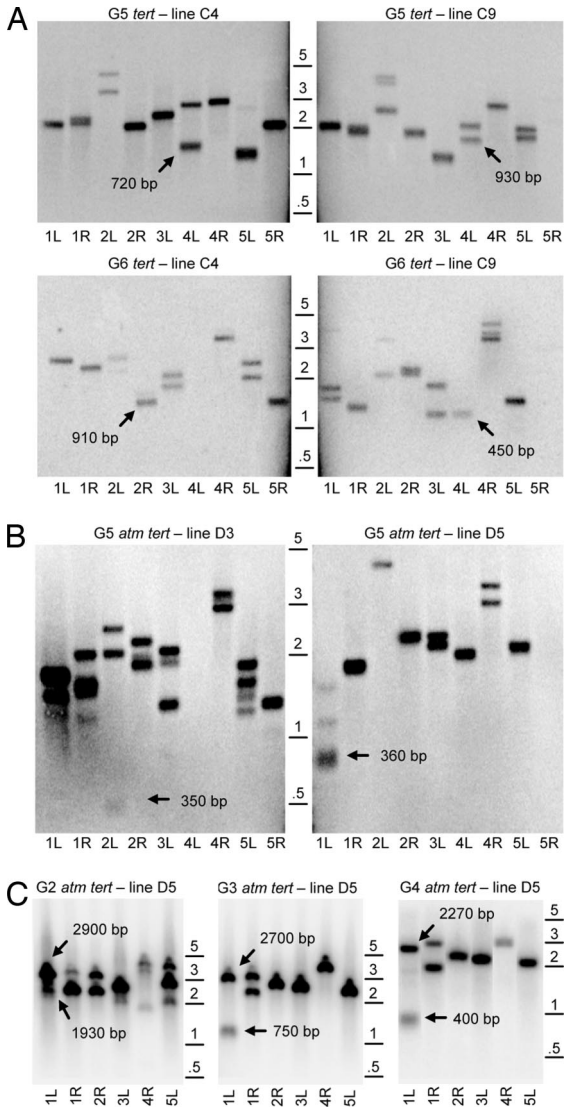

Fig. 2. A single critically shortened telomere in G_5 *atm tert* mutants. PETRA results for G_5 and G_6 *tert* plants (*A*) and G_5 *atm tert* mutants (*B*) are shown. The shortest telomere tract detected in each plant is indicated by an arrow. Sizes are relative to the position of the primer used for PETRA (35). Occasionally, PETRA reactions failed with 4L and 5R primers. (*C*) PETRA analysis of G_2–G_4 *atm tert* plants of line D5. The longest and shortest 1L telomeres are indicated by the arrows. Molecular size markers in kb are shown.

Table 2. Centromere signals in *tert* and *atm tert* mutants

Mutant	Line	Nuclei	No. of signals <10	No. of signals 10	No. of signals >10
Wild type		66	0	66 (100%)	0
G_5 *atm tert*	D5	66	17 (26%)	45 (68%)	4 (6%)
G_6 *tert*	69	51	13 (25%)	36 (71%)	2 (4%)
G_8 *tert*	69	71	31 (44%)	34 (48%)	6 (8%)

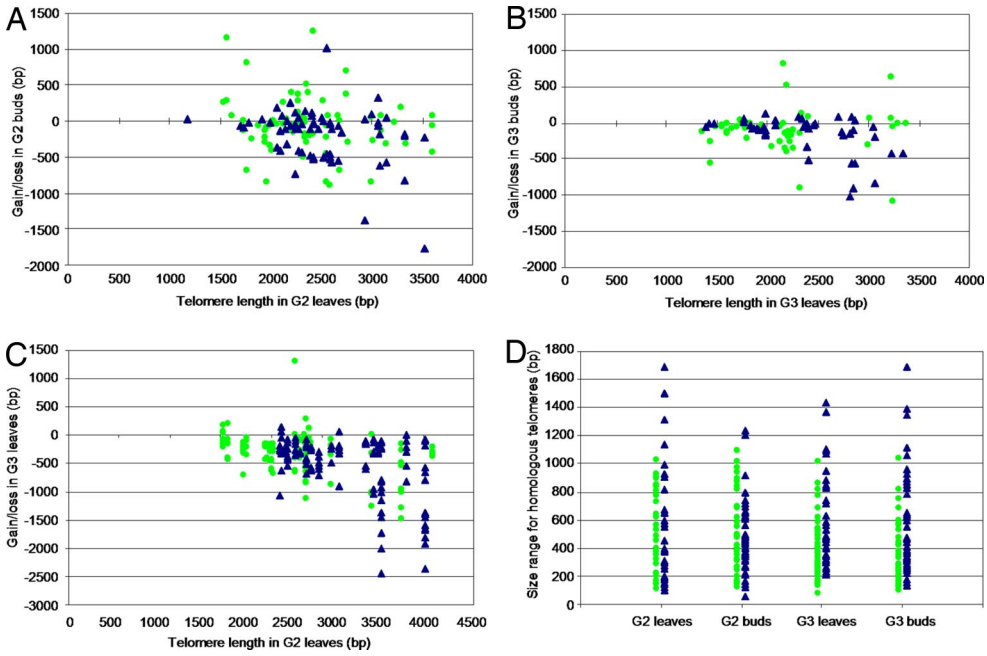

Fig. 3. ATM contributes to regulation of telomere length on individual chromosome ends. (*A–D*) Telomere dynamics in *tert* and *atm tert* mutants during G_2 and G_3. Green circles represent *tert*, and blue triangles represent *atm tert*. PETRA was performed on DNA from leaves (*x* axis) and floral buds (*y* axis) in G_2 mutants (*A*) and G_3 mutants (*B*), and the size difference between individual telomere tracts in the two organs was plotted. Values show measurements made in three to four plants per line, out of four individual lines (12–16 plants total). Size differences for individual telomeres in the leaves of G_2 parents and four G_3 progeny are plotted in *C*. Values on the *x* axis show the length of a particular telomere in the parent, and on the *y* axis the relative size differences of PETRA products generated for that same telomere in the progeny. For simplification, only parental chromosome ends displaying one telomere were analyzed. (*D*) Increased size range of telomeres on homologous chromosomes in *atm tert* mutants. Plotted are size differences between the longest and the shortest telomeres on homologous chromosome ends (defined as telomeres that give rise to only two comparable PETRA signals).

primer (Fig. 2 *A* and *B*). As the other telomeres that we could monitor were well above the minimal size threshold, we conclude that genome instability in G_5 *atm tert* mutants is triggered by the presence of a single critically shortened telomere.

TRD in *tert* and *atm tert* Mutants. We asked whether the very short telomeres in G_5 *atm tert* mutants were produced by TRD. TRD is a stochastic process in *Arabidopsis* that can lead to the loss of up to 1.5 kb of telomeric DNA in a single plant generation (6). Whereas such events are readily detected in early generations of *tert* (G_1, G_2), the frequency drops precipitously in later generations (G_6), indicating that longer telomeres are more susceptible to deletion. We found that a TRD event between the G_2 and G_3 generations of *atm tert* line D5 gave rise to a short 1L telomere (Fig. 2*C*). In G_2 *atm tert* mutants there was a tight cluster of 1L telomere tracts ranging from 1.9 to 2.9 kb, which migrated in the vicinity of rest of the telomeres in the population (Fig. 2*C*). In G_3, however, there were two strong hybridization signals for the 1L telomere, one at 2.7 kb and the other at 750 bp. Based on the intensity of hybridization, we suspect that the two bands represent telomeres on homologous chromosomes. Thus, one 1L telomere was subjected to the loss of either 1.2 or 2 kb in a single plant generation. The shorter 1L telomere was retained through G_4, although it dropped in size from 750 bp to 400 bp, consistent with attrition via the end replication problem (31). In G_5, the 1L telomere produced a more complex banding profile, indicating that it was subjected to an additional DNA processing event (Fig. 2*B*). These data indicate that ATM contributes to the regulation of telomere size.

ATM Affects Telomere Dynamics During Somatic Development and in Meiotic or Postmeiotic Tissues. Lustig and colleagues showed that yeast undergo both mitotic and meiotic TRD (10, 35). To ask whether TRD occurs during somatic development in *Arabidopsis*, we compared PETRA data from rosette leaves and floral buds isolated from a single plant. Plotted in Fig. 3*A* and B are the size differences for individual telomere tracts in G_2 and G_3 plants [supporting information (SI) Fig. 5]. Individual telomere tracts were highly dynamic, but in most samples the size difference was $<\pm 500$ bp. TRD is defined as the loss of >500 bp of telomeric DNA on a chromosome terminus in a single plant generation (6). Accordingly, telomeres in both *tert* and *atm tert* mutants were subject to TRD (Fig. 3 *A* and *B*). Although we found no difference in the relative amount of telomere truncation in G_3 plants, the two largest deletion events in G_2 (1.4 and 1.8 kb) were associated with *atm tert* mutants (Fig. 3 *A* and *B*).

Interestingly, in *tert*, but much more rarely in *atm tert*, we saw evidence for ALT (Fig. 3 *A* and *B*), defined here as a telomerase-independent telomere elongation event of >300 bp. When telomeres in G_2 leaves and G_2 buds were compared (Fig. 3*A*), 3% of the telomere tracts in *atm tert* mutants (2/66) showed ALT, whereas in *tert* this value rose to 12% (9/72) ($P = 0.04$). These findings suggest that ATM promotes ALT, and argue that ATM contributes to the regulation of both telomere elongation and telomere shortening events during somatic development.

To examine the effect of ATM on telomere dynamics in plants that have undergone meiosis, we plotted the size differences for individual telomeres from leaves in G_2 parents and their G_3 progeny (Fig. 3*C*). In this experiment, we gathered data from four progeny, and hence each parental telomere, whose size is plotted on the *x* axis, will give rise to a minimum of four signals in the progeny (plotted on the *y* axis). We detected only a single ALT event in *tert* (1/113), and none in *atm tert* (0/121) (Fig. 3*C*), suggesting that ALT may be primarily confined to mitotic cells. In contrast, many TRD events were observed; the largest of these events were found in *atm tert* mutants. Two of the longest parental telomeres in *atm tert* mutants (4.0 kb and 3.5 kb) gave rise to multiple PETRA signals in the progeny, which corre-

sponded to large truncations. Specifically, nine of these progeny telomeres derived from 2/5 *atm tert* parents showed TRD events >1.5 kb (9/121) ($P = 0.0003$). These data argue that the absence of ATM and TERT results in an accumulation of telomeres that have undergone TRD.

Deregulated Size Range Between Homologous Telomeres in *atm tert*. We next asked whether ATM plays a role in regulating telomere tracts on homologous chromosomes. For this experiment, we confined our study to PETRA reactions from G_2 and G_3 *atm tert* and *tert* samples that, for a given chromosome arm, gave rise to only two bands with a similar intensity (Fig. 3*D*). For the 165 pairs of telomeres examined in *tert* mutants, none showed a size range of $>\approx 1$ kb. The span was broader in *atm tert* mutants, with 11/179 homologous telomeres showing a size differential of >1.1 kb. 1L telomere tracts of grossly different sizes are also evident in the D5 *atm tert* line in G_3 (range = 2.0 kb) and G_4 (range = 1.9 kb) (Fig. 2*C*), indicating that these abnormal homologous telomeres were retained through two plant generations. We conclude that the absence of ATM and TERT leads to larger size differences between telomeres on homologous chromosomes.

Discussion

Telomere tracts are highly dynamic, and yet must be maintained above a minimal length threshold to safeguard genome stability. Here, we demonstrate that a single critically shortened telomere in G_5 *atm tert* leads to the formation of end-to-end sister chromatid fusions, accounting for the severe genome instability and early onset of the terminal phenotype in this mutant. Strikingly, for 2/3 *atm tert* lines, the telomere involved in the fusions was just above 300 bp, the minimal functional length defined for *Arabidopsis tert* mutants (34). In contrast, G_5 and even G_6 *tert* mutants do not harbor critically shortened telomeres and the chromosome fusion events that ultimately occur in these plants involve multiple chromosome ends. It is possible that dramatic telomere shortening events similar to the ones described for *Arabidopsis* trigger the early onset of genome instability in mice deficient in ATM and telomerase (26). TRD was not monitored in these animals.

The early onset of the terminal phenotype in *atm tert Arabidopsis* argues for an ATM-independent DNA damage checkpoint, which could be mediated by ATR; both ATM and ATR-dependent checkpoints have been described (20, 36). Supporting this idea is the absence of gross chromosomal rearrangements in *atm tert* mutants. Despite their terminal phenotype, mutants exhibit approximately the same level of aneuploidy as G_6 *tert* mutants, which are wild type in appearance. We hypothesize that the gross developmental abnormalities in G_5 *atm tert* mutants reflect the fact that all cells in the plant embryo inherit a critically shortened telomere. Although the plant developmental program is highly plastic and many cells are totipotent, once the critically shortened telomere fuses, there will be no neighboring cells with functional telomeres to compensate for the lost function.

Our data do not rule out the possibility that the early onset of genome instability in *atm tert* mutants reflects an ATM-mediated proliferative block for cells with critically shortened telomeres. Rather, we propose that ATM plays an additional, more direct role in promoting telomere length regulation on individual chromosome ends. Previous studies in mammals indicate that ATM negatively regulates intrachromosomal recombination and the formation of extrachromosomal telomeric DNA (37, 38), suggesting that ATM could play a role in TRD. However, we find only a modest increase in the number and magnitude of telomere deletion events in *atm tert* mutants. We hypothesize that ATM does not inhibit TRD *per se*, but instead is required to promote elongation of short telomeres generated by TRD (Fig. 4*A*). Supporting this conclusion are recent data from yeast indicating that ATM/TEL1 is required for telomerase recruitment to short telomeres (39, 40). Our data also suggest that ATM promotes ALT. Thus, ATM may play a generalized role in facilitating telomere maintenance.

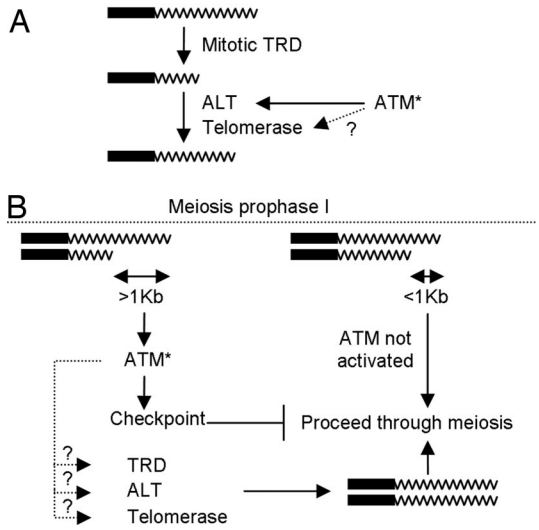

Fig. 4. Two models for ATM control of telomere length in *Arabidopsis*. (*A*) ATM ameliorates the consequences of mitotic TRD by promoting elongation of the short telomeres through ALT or telomerase. (*B*) ATM promotes resetting of telomeric length on homologous chromosomes in meiosis. ATM senses the size difference between the two telomeres when they are aligned in meiotic prophase I. Cells with homologous telomeres that are in a similar size range (≤1 kb difference) proceed through meiosis. If telomeres differ in size by >1 kb, an ATM-dependent checkpoint is activated (ATM*) that blocks meiotic progression. The block could be alleviated through ATM signaling to telomerase or to recombinational machinery (ALT) to elongate the shorter telomere of the pair. Alternatively, the longer telomere could be subjected to TRD.

Whereas ATM deficiency leads to complete sterility in mammals (41), it manifests as only a partial sterility defect in *Arabidopsis* (42), enabling us to investigate the consequences of ATM inactivation in vegetative and in meiotic and postmeiotic cells. We found unusually large deletions in the telomere tracts of *atm tert* mutants that had undergone meiosis. Precisely when TRD occurs during plant development is unknown. Telomere tracts may undergo a low level of mitotic TRD throughout vegetative growth, but such isolated events would go undetected in our PETRA assay. However, if a chromosome end in the germ cell lineage suffered TRD, the shortened telomere would have a high probability of being inherited by progeny plants, and thus would be detected in our assay. It is also possible that TRD occurs in meiosis.

A second important conclusion from our study is that telomeres on homologous chromosome ends display greater size ranges in *atm tert* relative to *tert* mutants, implying that ATM functions in an additional checkpoint capacity to monitor telomere length on homologous chromosomes. Data from yeast implicate meiotic telomere clustering in the resetting of artificially long telomeres by TRD (10, 11). When homologous chromosomes align during prophase I, there is an opportunity to directly compare the telomere tracts on the two homologues. As illustrated in Fig. 4*B*, homologous telomeres in *Arabidopsis* are normally maintained within a size range of ≈1 kb. We hypothesize that a larger size differential activates an ATM-dependent checkpoint, triggering cell cycle arrest. Meiotic cells harboring telomeres of grossly different lengths would accumulate in the absence of ATM, a prediction consistent with the early appearance of a critically shortened telomere in *atm tert* mutants. Further investigation is needed to determine whether *Arabidopsis* can abrogate this checkpoint by resetting telomere length on

GENETICS

homologous chromosome ends through meiotic telomerase action or ALT on shorter telomeres or TRD on longer ones, but this possibility is intriguing.

A mechanism that monitors telomere tracts on homologous chromosomes could not only circumvent the devastating consequences invoked by a critically shortened telomere, but also would allow progeny to inherit telomeres of the same length. Over evolutionary time, this latter advantage could be substantial.

Materials and Methods

Plant Material and Growth Conditions. The same four lines produced in (30) from the same cross between plants heterozygous for *tert* and *atm* were used here (SI Fig. 5). For all experiments, *atm tert* and *tert* seeds were planted the same day and grown in the same chamber at 23°C using a 16 h/8 h photoperiod.

FISH. Bacterial artificial chromosomes (BACs) were used as FISH probes for individual termini from fixed pistils (32). Repeated bicolor FISH was performed with probes labeled with either SpectrumGreen-dUTP (Vysis no. 30-8003200) or Cy3-dUTP (Amersham Pharmacia Biotech) using standard nick translation reactions. For analysis of lines D3 and F11, the 5S and 25S rDNA probes correspond to clones CD3-1 (TAIR stock no. 2540232) and CD3-196 (TAIR stock no. 2540222), respectively, and were labeled by nick-translation (43) using Texas red-dUTP (C-7631; Invitrogen) and dUTP-AlexaFluor488-dUTP (C-11397; Invitrogen), respectively. Telomere tracts were detected by using a peptide nucleic acid (PNA) probe (C3TA3)2 labeled with Cy3 (Applied Biosystems).

PETRA. Genomic DNA from *tert* and *atm tert* samples was extracted the same day (30) and resuspended at 100 ng/μl. PETRA was as described in ref. 6, except that two primers were added to amplify the 2L and 4L telomeres (33): 5′-TTCGCTCGCCGTTACTAAGGGAAT-3′ for 2L-R9 and 5′-TCCTTGGATGTGGTAGCCGTTTCT-3′ for 4L-R3, located in the 25S and 18S rDNA genes, respectively. Telomere size was calculated by subtracting the distance of the subtelomeric primer binding site from the observed size of the PETRA product using ImageQuant software (Molecular Dynamics).

We thank Jon Lamb for help with FISH experiments, Greg Copenhaver for advice on designing 2L and 4L probes for PETRA, Aude Vespa for discussion, and Art Lustig, Matt Watson, and Karel Riha for insightful comments on the manuscript. This work was supported by National Science Foundation Grant MCB 0615928 (to D.E.S.) and Czech Science Foundation Grant 522/06/0380 (to J.S.).

1. de Lange T (2005) *Genes Dev* 19:2100–2110.
2. de Lange T (2002) *Oncogene* 21:532–540.
3. Teixeira MT, Arneric M, Sperisen P, Lingner J (2004) *Cell* 117:323–335.
4. Hemann MT, Strong MA, Hao LY, Greider CW (2001) *Cell* 107:67–77.
5. Henson JD, Neumann AA, Yeager TR, Reddel RR (2002) *Oncogene* 21:598–610.
6. Watson JM, Shippen DE (2007) *Mol Cell Biol* 27:1706–1715.
7. Bhattacharyya MK, Lustig AJ (2006) *Trends Biochem Sci* 31:114–122.
8. Lustig AJ (2003) *Nat Rev Genet* 4:916–923.
9. Kyrion G, Boakye KA, Lustig AJ (1992) *Mol Cell Biol* 12:5159–5173.
10. Joseph I, Jia D, Lustig AJ (2005) *Curr Biol* 15:231–237.
11. Joseph I, Lustig AJ (2007) *Cell Mol Life Sci* 64:125–130.
12. Williams B, Bhattacharyya MK, Lustig AJ (2005) *DNA Repair (Amsterdam)* 4:994–1005.
13. Wang RC, Smogorzewska A, de Lange T (2004) *Cell* 119:355–368.
14. Compton SA, Choi JH, Cesare AJ, Ozgur S, Griffith JD (2007) *Cancer Res* 67:1513–1519.
15. Verdun RE, Crabbe L, Haggblom C, Karlseder J (2005) *Mol Cell* 20:551–561.
16. Verdun RE, Karlseder J (2006) *Cell* 127:709–720.
17. Gallego ME, White CI (2005) *Chromosome Res* 13:481–491.
18. d'Adda di Fagagna F, Teo SH, Jackson SP (2004) *Genes Dev* 18:1781–1799.
19. Harrison JC, Haber JE (2006) *Annu Rev Genet* 40:209–235.
20. Culligan KM, Robertson CE, Foreman J, Doerner P, Britt AB (2006) *Plant J* 48:947–961.
21. Karlseder J, Hoke K, Mirzoeva OK, Bakkenist C, Kastan MB, Petrini JH, de Lange T (2004) *PLoS Biol* 2:E240.
22. Kishi S, Lu KP (2002) *J Biol Chem* 277:7420–7429.
23. Greenwell PW, Kronmal SL, Porter SE, Gassenhuber J, Obermaier B, Petes TD (1995) *Cell* 82:823–829.
24. Pandita TK (2001) *Radiat Res* 156:642–647.
25. Wong KK, Maser RS, Bachoo RM, Menon J, Carrasco DR, Gu Y, Alt FW, DePinho RA (2003) *Nature* 421:643–648.
26. Qi L, Strong MA, Karim BO, Armanios M, Huso DL, Greider CW (2003) *Cancer Res* 63:8188–8196.
27. Chan SW, Blackburn EH (2003) *Mol Cell* 11:1379–1387.
28. Bi X, Wei SC, Rong YS (2004) *Curr Biol* 14:1348–1353.
29. Silva E, Tiong S, Pedersen M, Homola E, Royou A, Fasulo B, Siriaco G, Campbell SD (2004) *Curr Biol* 14:1341–1347.
30. Vespa L, Couvillion M, Spangler E, Shippen DE (2005) *Genes Dev* 19:2111–2115.
31. Riha K, McKnight TD, Griffing LR, Shippen DE (2001) *Science* 291:1797–1800.
32. Mokros P, Vrbsky J, Siroky J (2006) *Genome* 49:1036–1042.
33. Copenhaver GP, Pikaard CS (1996) *Plant J* 9:259–272.
34. Heacock M, Spangler E, Riha K, Puizina J, Shippen DE (2004) *EMBO J* 23:2304–2313.
35. Li B, Lustig AJ (1996) *Genes Dev* 10:1310–1326.
36. Culligan K, Tissier A, Britt A (2004) *Plant Cell* 16:1091–1104.
37. Hande MP, Balajee AS, Tchirkov A, Wynshaw-Boris A, Lansdorp PM (2001) *Hum Mol Genet* 10:519–528.
38. Drexler GA, Wilde S, Beisker W, Ellwart J, Eckardt-Schupp F, Fritz E (2004) *DNA Repair (Amsterdam)* 3:1345–1353.
39. Goudsouzian LK, Tuzon CT, Zakian VA (2006) *Mol Cell* 24:603–610.
40. Sabourin M, Tuzon CT, Zakian VA (2007) *Mol Cell* 27:550–561.
41. Xu Y, Ashley T, Brainerd EE, Bronson RT, Meyn MS, Baltimore D (1996) *Genes Dev* 10:2411–2422.
42. Garcia V, Bruchet H, Camescasse D, Granier F, Bouchez D, Tissier A (2003) *Plant Cell* 15:119–132.
43. Yu W, Lamb JC, Han F, Birchler JA (2007) *Genetics* 175:31–39.